Jurnal Farmasi dan Ilmu Kefarmasian Indonesia
Pharmacy and Pharmaceutical Sciences Journal
Published by Faculty of Pharmacy Universitas Airlangga
OPEN ACCESS
E-ISSN 2580-8303
P-ISSN 2406-9388

Jurnal Farmasi dan Ilmu Kefarmasian Indonesia Vol. 12 No. 2 August 2025, 161-172
DOI: 10.20473/jfiki.v12i22025.161-172
Available online at https://e-journal.unair.ac.id/JFIKI/

Optimization and Stability Assessment of Clindamycin HCl Transethosome: Exploring the Effects of Ethanol and Tween 80 Concentrations

Annisa Amriani, Adik Ahmadi, Muhammad Arif Maulana, Fariz Alfarrazi, Elsa Fitria Apriani*
Department of Pharmacy, Faculty of Mathematics and Natural Sciences, Universitas Sriwijaya, Indralaya, Indonesia

*Corresponding author: elsafitria@mipa.unsri.ac.id
Orcid ID: 0000-0002-0403-8458

Submitted: 4 December 2024
Revised: 24 June 2025
Accepted : 27 August 2025

Abstract

Background*: Clindamycin HCl is drug commonly used as an anti-acne in conventional topical formulations. However, effectiveness of clindamycin HCl in conventional topical formulations is limited due to poor skin penetration, whereas Propionibacterium acnes colonies in the deeper sebaceous follicle area. To overcome this limitation, transethosome emerged as an innovative drug delivery system capable of enhancing drug permeation through the skin.* ***Objective:*** *This study aimed to optimise clindamycin HCl transethosome formula using a 2^2-factorial design.* ***Methods:*** *The optimisation was carried out with two factors and two levels, ethanol (20% and 40%) and Tween 80 (15% and 25%), on the responses of particle size, polydispersity index, and entrapment efficiency. Transethosomes were prepared using the thin-layer hydration method. Furthermore, the optimum transethosomes were tested for stability using the ICH Q1A(R2) method.* ***Results:*** *The optimum formula contains 20% ethanol and 15% Tween 80. The optimum transethosome shows a particle size of 240.933 ± 1.488 nm, a polydispersity index (PDI) of 0.177 ± 0.013, and an entrapment efficiency (EE) of 89.401 ± 0.118%. The release model follows zero-order kinetics with an activation energy of 2.978758 cal/mol. The shelf life at 25°C ± 2°C / RH 60% ± 5% is 22.536 days, and at 5°C ± 3°C is 24.572 days.* ***Conclusion:*** *The optimum transethosomal formula of clindamycin HCl exhibited good initial physical characteristics, with particle size below 250 nm, polydispersity index (PDI) of less than 0.3, and high entrapment efficiency (EE). However, the low shelf life indicated a need for further optimisation to achieve long-term stability.*

Keywords: *clindamycin HCl, optimization, stability, transethosomes*

How to cite this article:
Amriani, A., Ahmadi, A., Maulana, M. A., Alfarrazi, F. & Apriani, E. F. (2025). Optimization and Stability Assessment of Clindamycin HCl Transethosome: Exploring the Effects of Ethanol and Tween 80 Concentrations. *Jurnal Farmasi dan Ilmu Kefarmasian Indonesia*, 12(2), 161-172. http://doi.org/10.20473/jfiki.v12i22025.161-172

P-ISSN: 2406-9388
E-ISSN: 2580-8303

INTRODUCTION

Clindamycin is a topical antibiotic with bacteriostatic and anti-inflammatory properties, commonly used to treat acne (Dawson & Dellavalle, 2013). However, clindamycin in conventional topical formulations faces challenges in achieving adequate skin penetration, with studies reporting only about 5-8% of the active ingredient being absorbed into the deeper skin layers (Abdellatif & Tawfeek, 2016). Additionally, clindamycin faces challenges in penetrating the skin's stratum corneum. In contrast, *Propionibacterium acnes*, the bacterium responsible for acne, resides in the sebaceous glands located in the dermis, necessitating deeper skin penetration to reach the target cells (Dréno, 2017; Mollerup et al., 2016). Therefore, developing an effective drug delivery system, such as transethosomes, is essential.

Transethosomes have been shown to exhibit enhanced vesicle elasticity, which contributes to their superior deformability and, consequently, improved skin permeation, as demonstrated by Garg et al. (2017), in comparison to other nanovesicles. This improvement is attributed to the combination of ethanol and surfactants, which cause structural rearrangements in the lipid bilayer of the vesicles (Ascenso et al., 2015; Kumar et al., 2019). Moreover, transethosomes offer better stability than ethosomes, as evidenced by Esposito et al. (2022), who found that the higher lipid and surfactant content in transethosome formulations contributes to increase steric stability.

The selection of appropriate surfactants and ethanol concentrations is critical in formulating transethosomes. Factorial design is a valuable approach for optimizing all influencing parameters simultaneously, allowing for assessing each factor's effect and interactions. This design reduces the number of trials, time, and costs while providing reliable results. Compared to one-factor-at-a-time experiments, factorial design is more efficient and can detect interactions, making it ideal for this study (Elhalil et al., 2016; Watkins & Newbold, 2020).

The surfactant used in this study was Tween 80. According to Zeb et al. (2016), Tween 80 demonstrates superior deformability and skin permeation compared to sodium cholate. Additionally, El-Laithy et al. (2011) found that Tween 80 offers better entrapment of active ingredients than Span 80, likely due to its longer carbon chain. Ethanol is a crucial excipient optimised in transethosome formulations due to its primary role as a skin penetration enhancer. It works by fluidising the intercellular lipids of the stratum corneum, the outermost layer of the skin, thereby creating temporary pathways that facilitate drug penetration. However, optimising ethanol concentration is critically essential; an inappropriate concentration can compromise the integrity of the transethosome vesicles, leading to drug leakage and reduced entrapment efficiency (Abdulbaqi et al., 2016; Li et al., 2012; Rakesh & Anoop, 2012). Therefore, while Apriani et al. (2023) successfully optimised the ethanol concentration to 40% for clindamycin HCl ethosome systems, achieving high entrapment efficiency, a particle size of less than 200 nm, and a polydispersity index of less than 0.4, specific research on the optimal ethanol concentration for clindamycin HCl transethosomes is yet to be established.

Stability testing is crucial for confirming the quality of pharmaceutical products over time, as environmental conditions like humidity, temperature, and light affect their stability. This testing helps determine the retest period, shelf life of drugs, and storage recommendations (ICH, 2023). The ICH Q1A(R2) guidelines, developed by the FDA, align storage conditions with climatic zones, categorizing regions into four zones. Indonesia falls into Zone IVB, characterized by hot and humid conditions, necessitating accelerated testing. The scientific basis for modelling accelerated test data is the Arrhenius kinetic equation, which predicts the degradation of active ingredients influenced by temperature and humidity. This model analyzes the impact of humidity, time, and temperature on degradation rates, yielding more precise predictions than traditional accelerated testing methods, which assume a linear correlation between temperature and degradation. The reaction kinetics offer a more precise estimation of degradation rates, and the stability of a product can be predicted using kinetic constants, where lower constants correlate with longer stability (Clancy et al., 2017).

Based on the description above, transethosome system was optimized using Tween 80 as the surfactant and 96% ethanol as the penetration enhancer. The concentration of Tween 80, initially set at 20% in previous studies, was modified to 15% and 25% of the total lipid content. Ethanol concentrations of 20% and 40% were selected based on prior research. This combination results in four transethosome formulations using the 2^2 factorial design model. The formulations were evaluated based on particle size, polydispersity index, and entrapment efficiency with the data processed using Design Expert 12® software to identify the optimum formula. The optimum formula was then

P-ISSN: 2406-9388
E-ISSN: 2580-8303

subjected to accelerated stability testing over two months, with the results analyzed using SPSS software.

MATERIALS AND METHODS

Materials

Clindamycin HCl (gift from PT. Dexa Medica, Palembang, Indonesia), Phospholipon 90G (Lipoid®, Ludwigshafen, Germany), methanol (Merck®, Indonesia), dichloromethane (Merck®, Indonesia), Tween 80 (Merck®, Indonesia), KH2PO4 (Merck®, Indonesia), NaOH (Merck®, Indonesia), distilled water (Bratachem, Indonesia), 96% ethanol (Merck®, Indonesia), and propylene glycol (DOW®, Australia) were the materials used for this study.

Method

Tools

The tools used in this study included an analytical balance (NewTech Electronic Balance®), Rotary Evaporator (Dragon Lab®), Magnetic Stirrer (IKA® C-MAG HS 4), Oven (Memmert®), Refrigerator (Sanyo®), micropipette 100-1000 µl (Dragon Lab®), UV-Vis Spectrophotometer (Biobase® BK-UV1900PC), Particle Size Analyzer (Malvern® Zetasizer), pH meter (Lutron® pH Electrode PE-03), Sonicator Bath (GT SONIC®), Ultra-Turrax (Ika® T-25 Digital Ultra Turrax), Centrifuge (DLAB©: D2012 PLUS), Climatic Chamber 25°C/60% RH (Thermolab® Scientific Equipment), Walk-In Climatic Chamber 30°C/75% RH (Thermolab® Scientific Equipment), Climatic Chamber 40°C/75% RH (Maximus®), and glassware (Pyrex®).

Optimization of the clindamycin HCl transethosomal formula

This study made a transethosomes formulation containing clindamycin HCl using a 2^2-factorial design with variations concentrations in ethanol and tween 80 (Apriani et al., 2023). The formulation design of clindamycin HCl transethosomes can be seen in Table 1.

Production of clindamycin HCl transethosomes

Clindamycin HCl transethosomes were made following the research of Apriani et al. (2019) with slight modifications. The rotary evaporator was operated in a vacuum at 54°C with an initial rotation speed of 50 rpm and a maximum rotational speed of 125 rpm to produce thin films from a mixture of Phospholipon 90G, tween 80, and organic solvents dichloromethane and methanol. The round bottom flask was sealed with aluminum foil and cooled for 24 hours after the thin layer was formed. The hydration solution was prepared from a mixture of clindamycin HCl, propylene glycol, ethanol, and phosphate buffer pH 7.4. A clindamycin HCl transethosomes suspension was generated by hydrating the samples in a rotary evaporator at 37°C without a vacuum. The obtained clindamycin HCl transethosomes suspension was then reduced in particle size using ultra turrax for 15 minutes at a speed of 7600 rpm. Subsequently, the suspension was subjected to sonication for three cycles, each running for 10 minutes.

Transetosome characterization

Percentage of entrapment efficiency

The entrapment efficiency test (%EE) was conducted at 15000 rpm, 4°C for 30 mimutes using the indirect method. The suspension of transethosomes will be divided into two phases: entrapped and non-entrapped. The absorbance value was subsequently determined through using a UV-Vis spectrophotometer at 204 nm to measure the non-entrapped phase (Apriani et al., 2023). Free clindamycin HCl levels were calculated based on the previously obtained regression equation. Equation 1 is employed to determine the entrapment efficiency (%EE).

$$\%EE = \left[\frac{(Qt-Qs)}{Qt}\right] x100\% \quad \text{..... (Equation 1)}$$

Note:

%EE : Entrappment Efficiency (%)

Qt : Total clindamycin HCl concentration in transethosomes suspension (µg/mL)

Qs : Clindamycin HCl concentrations that are not entrapped in the transethosomes suspension (µg/mL).

Table 1. Clindamycin HCl transethosomes formulations

Ingredient	Concentration (%)			
	F1	F2	F3	F4
Clindamycin HCl	1	1	1	1
Phospolipon 90G	2	2	2	2
Propylene Glycol	5	5	5	5
Ethanol	20	40	40	20
Tween 80	25	25	15	15
Phosphate Buffer pH 7,4	up to 100 mL	up to 100 mL	up to 100 mL	up to 100 mL

P-ISSN: 2406-9388
E-ISSN: 2580-8303

Particle size and polydispersity index

The Dynamic Light Scattering (DLS) method was employed to determine the polydispersity index and particle size using a Particle Size Analyzer (PSA). The sample was dissolved in 10 ml of phosphate buffer pH 7.4 and then was transferred to a cuvette for measurement (Apriani et al., 2022; Mardiyanto et al., 2023).

Optimum formula determination

The results of the characterization are used to determine the optimum transethosome formula. The Design-Expert 12® software was employed to identify the most optimized formula, which had a desirability value near one. The optimum formula was determined by the following criteria: a polydispersity index value of less than 0.3, a particle size within the 80-250 nm range, and the maximum percentage of drug entrapment efficiency within the formula (Ferrara et al., 2022; Raj et al., 2023).

Stability study

Stability testing followed the guidelines written by ICH (2003) with the accelerated test method. Physical stability testing was conducted using a climatic chamber with three storage conditions. The storage conditions used were 40ºC±2ºC/75% RH±5%, 30ºC±2ºC/75% RH±5% and 25ºC±2ºC/60% RH±5%. Organoleptic (discolouration and phase separation), entrapment efficiency, and pH were conducted on the tested samples on days 0, 22, and 44. Then, the shelf life is calculated using the formula according to the release kinetics model.

Data on the decrease in entrapment efficiency obtained from the ICH Q1A(R2) stability test are used to calculate the kinetic constant by examining the coefficient of determination (R2) in close proximity to one. The summary of the release kinetics model formula can be seen in Table 2.

Table 2. Release kinetics equation

Release Kinetic	Equation
Zero-Order	$C = K_o.t$
First-Order	$\ln C = K_1.t$
Higuchi	$C = K_h.\ t^{1/2}$
Korsmeyer's Peppas	Ln C = n. ln t + ln K

Note:
C = The concentration of drug released at time t
K_0, K_1, K_h, K = Drug release constant
N = Drug diffusion exponent

The Arrhenius equation is acquired by plotting the Arrhenius 1/T vs Log K graph in accordance with the release kinetics that were obtained. The K and Ea values, which indicate the decomposition rate of the vesicles and the minimum energy required for the reaction to occur, are determined using these equations. The K value is obtained by substituting the Log K value from the equation Log K = Log A - (Ea/(2.303 R))x 1/T according to the temperature of the storage conditions. The K value is subsequently employed to determine the shelf life (Dlamini et al., 2019; Lu & Ten Hagen, 2020).

Data analysis

Design-Expert 12® program was employed to conduct data analysis in order to determine the impact of ethanol concentration and Tween 80, as well as their interaction, on the characteristics of the transethosome suspension which resulted. The parameters used to determine the optimum formula are R2, predicted R2, adjusted R2, adequate precision, and p-value. SPSS 25 software is used to process transethosomes stability data that has been tested.

RESULTS AND DISCUSSION

The thin-film hydration method was used to produce clindamycin HCl transethosomes. The obtained transethosome suspension, shown in Figure 1, was milky white with a distinct ethanolic odor consistent across all formulations. This suspension was stored it in the cold temperature (2-8ºC), before further characterization.

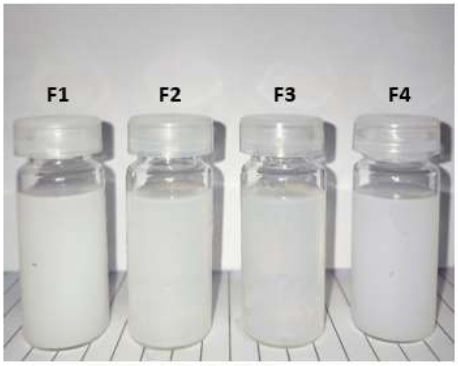

Figure 1. Clindamycin HCl transethosomal suspension at Day-0

Characterization of the Clindamycin HCl transethosomes involved parameters such as entrapment efficiency, particle size, and polydispersity index (PDIs), which are critical for identifying the optimum formula. The transethosomes are considered optimal if they exhibit high entrapment efficiency, particle sizes between 80-250 nm, and a PDIs below 0.3 (Ferrara et al., 2022). Table 3 summarizes the characterization results, which indicate that all formulations met the criteria for satisfactory particle sizes (203-265 nm), PDIs (0.15-0.23), entrapment efficiencies (81-89%).

P-ISSN: 2406-9388
E-ISSN: 2580-8303

Table 3. Characterization results of clindamycin HCl transetosomes

Formula	Entrapment Efficiency (%)	Particle Size (nm)	Polydispersity Index
F1	87.736±0.140	265.467±2.088	0.233±0.003
F2	81.675±0.438	203.067±1.312	0.152±0.010
F3	82.871±0.139	209.800±1.157	0.160±0.039
F4	89.401±0.118	240.933±1.488	0.177±0.013

Note: Data are given as mean±SD, n=3

Table 4. Model analysis result

Parameter	*p-value*	Adjusted R^2	Predicted R^2	The difference between Adjusted R2 and Predicted R2	Adequate Precision
Entrapment Efficiency	<0.0001*	0.9920	0.9869	0.0051	44.1205
Particle Size	<0.0001*	0.9947	0.9914	0.0033	56.8448
Polydispersity Index	0.0232*	0.5551	0.2719	0.2832	5.2560

Note: * showed significant results (p<0.05)

Table 5. Responses analysis result

Parameter		Intercept	A (Tween 80)	B (Ethanol)	AB (Interaction)
Entrapment Efficiency	Coefficient	85.42	-0.7152	-3.15	0.1172
	P-Value		<0.05*	<0.05*	0.217
	%Contribution		4.87408	94.4107	0.130841
Particle Size	Coefficient	229.82	4.45	-23.38	-7.82
	P-Value		<0.0001*	<0.0001*	<0.0001*
	%Contribution		3.14279	86.7777	9.69702

Note: * showed significant results (p<0.05)

To determine the optimum formulation, Design-Expert 12® software was used, considering model and response analysis. The model is considered satisfactory if it fulfills the following criteria: a p-value of less than 0.05, an adjusted R^2 in excess of 0.7, a difference between the adjusted and predicted R^2 of less than 0.2, and a precision of at least 4 (Miksusanti et al., 2023). The model analysis results of the three parameters can be seen in Table 4.

The entrapment efficiency and particle size parameters satisfy the criteria for a satisfactory model, as indicated in Table 4. Nevertheless, the polydispersity index fails to satisfy these criteria, as its adjusted R^2 value and the difference between the adjusted R^2 and predicted R^2. The adjusted R^2 is used because the model includes multiple independent variables, namely ethanol and Tween 80. This value reflects the proportion of variability in the response variable explained by the model, representing the sample population. The model explains 99.20% to 99.47% of the population variance for entrapment efficiency and particle size, respectively, as indicated by the adjusted R^2 values of 0.9920 and 0.9947. This data suggests a robust linear relationship between the dependent variables and the independent variables.

The predicted R^2 parameter reflects the ideal model fit and indicates how closely the regression obtained from the experimental responses matches the regression predicted by the system. The predicted R^2 values for entrapment efficiency and particle size are 0.9869 and 0.9914, respectively, meaning that the observed regression closely aligns with the expected regression by 98.69% and 99.14%. The modeling error is represented by the difference between the adjusted R^2 and predicted R^2. The differences between entrapment efficiency and particle size are 0.0051 and 0.0033, respectively, suggesting a small modeling error. Additionally, the model's robustness and resistance to disturbance are suggested by a precision value that exceeds 4. The dependent variables—entrapment efficiency and particle size—are substantially influenced by the independent variables, as indicated by these results. Consequently, these two parameters are eligible for further optimization process analysis.

Response analysis was conducted to evaluate the effects of the ethanol factor, Tween 80, and their interaction on the entrapment efficiency and particle size parameters. The coefficient, p-value, and percentage contribution of each factor can be used to evaluate the response analysis results. The detailed response analysis results are presented in Table 5 and Figure 2.

P-ISSN: 2406-9388
E-ISSN: 2580-8303

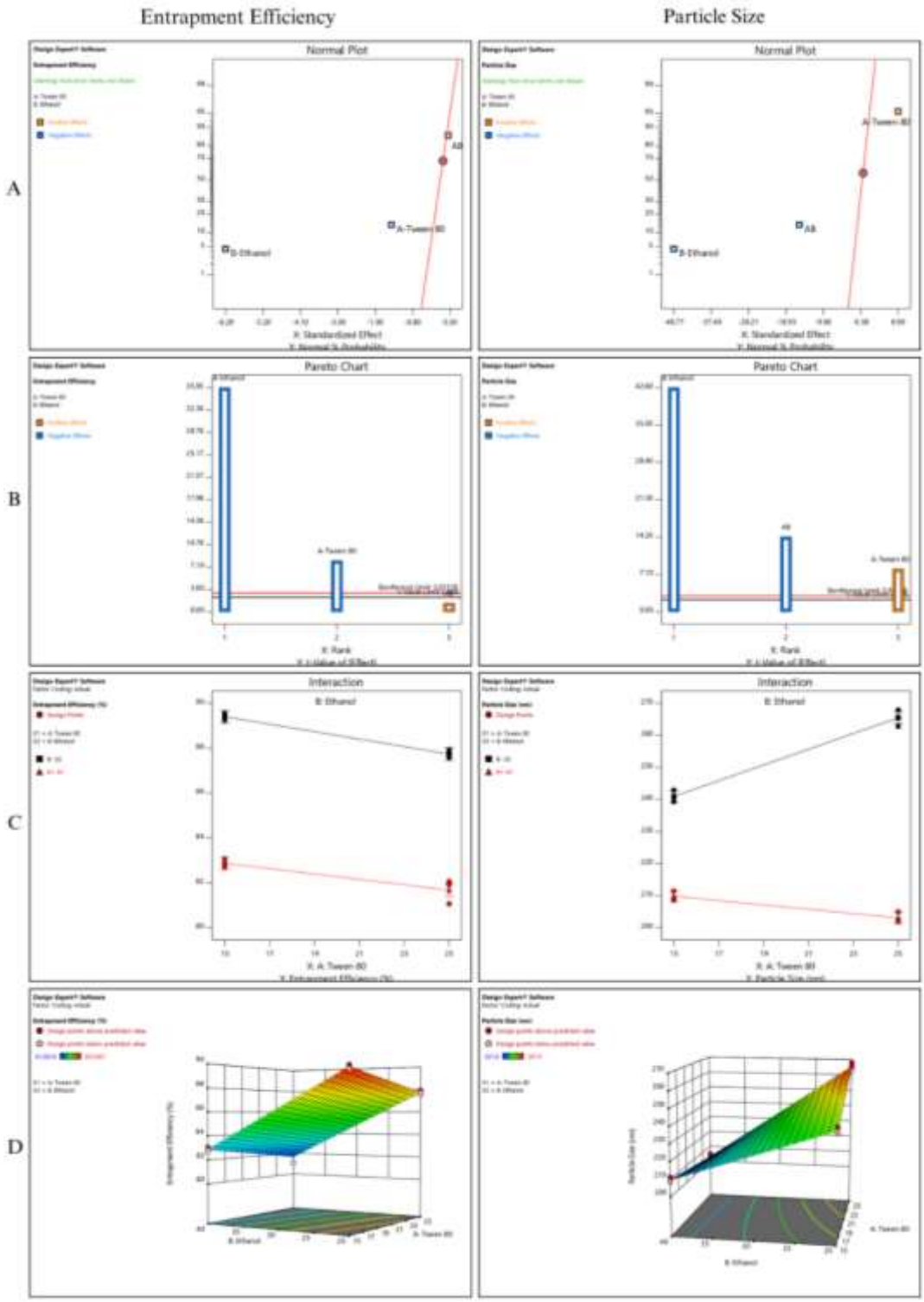

Figure 2. Normal plot (A), pareto chart (B), interaction (C) and 3d surface (D) graphs of entrapment efficiency and particle size parameters

The response analysis, detailed in Table 5 and Figure 2, showed that both ethanol and Tween 80 significantly affected entrapment efficiency and particle size, with their interaction notably influencing particle size ($p<0.05$). Figures 2A and 2B support these findings, showing that the interaction between Tween 80 and ethanol did not significantly affect entrapment efficiency but significantly impacted particle size. The Pareto chart further emphasized that ethanol had the highest contribution, with 94.41% and 86.78% for entrapment efficiency and particle size, respectively.

The interaction between Tween 80 and ethanol is shown in Figure 2C. For entrapment efficiency, the interaction curves do not intersect, indicating no

P-ISSN: 2406-9388
E-ISSN: 2580-8303

interaction between the factors, which is supported by the p-value for interaction between Tween 80 and ethanol on entrapment efficiency, showing no significant effect. In contrast, for particle size, the curves intersect, indicating an interaction between Tween 80 and ethanol, as confirmed by the significant p-value for interaction between Tween 80 and ethanol on particle size. The black line represents low ethanol concentration, while the red line represents high ethanol concentration. At low ethanol concentrations, increasing Tween 80 concentration decreases entrapment efficiency and increases particle size. These results are additionally confirmed by the 3D surface graph in Figure 2D, which shows that the red area represents the highest entrapment efficiency and the blue area represents the smallest particle size.

The influence of factors on entrapment efficiency and particle size can be both positive and negative, as indicated by the coefficients in Table 5. The entrapment efficiency was negatively impacted by ethanol and Tween 80, as indicated by a negative coefficient (-). Specifically, increasing the concentration of ethanol led to a decrease in entrapment efficiency. The highest entrapment efficiency was observed in F4, with concentrations of 96% ethanol and Tween 80 at 20% and 15%, respectively. This result aligns with studies by Bendas & Tadros (2007), and Zhou et al. (2010), which reported that while ethanol concentration generally increases entrapment efficiency up to a certain point, excessive ethanol can cause vesicle instability, leading to decreased entrapment due to leakage of the bilayer coating.

Additionally, lower surfactant concentrations in F4 resulted in higher entrapment efficiency, which corroborates findings by Varia et al. (2022), and Wu et al. (2019). High surfactant concentrations tend to cause vesicle leakage, decreasing drug entrapment efficiency. This is because surfactants enhance vesicle flexibility, increase leakage, and can also lead to micelle and pore formation when their concentration exceeds the critical lamellar transition temperature (Bnyan et al., 2018). In terms of particle size, ethanol and its interaction with other factors had a negative effect, while Tween 80 showed a positive influence. As supported by Somwanshi (2019), Monisha et al. (2019), and Pathan et al. (2016), increasing ethanol concentration reduced vesicle size, likely due to ethanol's ability to penetrate the vesicular bilayer, reducing its thickness. In contrast, higher concentrations of Tween 80 led to smaller particle sizes. This finding is consistent with Varia et al. (2022) and Iskandarsyah et al. (2020), who noted that Tween 80's smaller HLB value and ability to form hydrogen bonds with the phospholipid bilayer facilitate a reduction in particle size. Table 3 summarizes the optimization process, which suggested an optimum formula consisting of 15% of tween 80 and 20% of 96% ethanol. This formula achieved a particle size of 240.93 ± 1.49 nm, a PDI of 0.18 ± 0.01, and entrapment efficiency of 89.40 ± 0.12%.

The stability of this formula was then tested according to ICH Q1A (R2) guidelines at various storage conditions. The results, as shown in Table 6 and Figure 3, indicate that storage at higher temperatures led to color changes (from white to yellowish) and the formation of precipitates, particularly at 40°C. This suggests lipid vesicle breakdown and oxidation.

Table 6. Organoleptic results of stability test in optimum formula

Day	Storage Condition	Result
0	25ºC±2ºC/60% RH ± 5% RH	Clear white colour, ethanol aroma, no precipitate
	30ºC±2ºC/75% RH ± 5% RH	Clear white colour, ethanol aroma, no precipitate
	40ºC±2ºC/75% RH ± 5% RH	Clear white colour, ethanol aroma, no precipitate
22	25ºC±2ºC/60% RH ± 5% RH	Clear white colour, odorless, precipitate
	30ºC±2ºC/75% RH ± 5% RH	Clear white colour, odorless, precipitate
	40ºC±2ºC/75% RH ± 5% RH	Clear white colour, odorless, precipitate
44	25ºC±2ºC/60% RH ± 5% RH	Slightly yellowish in colour, odorless, precipitate
	30ºC±2ºC/75% RH ± 5% RH	Slightly yellowish in colour, odorless, precipitate
	40ºC±2ºC/75% RH ± 5% RH	Yellow in colour, odorless, precipitate

P-ISSN: 2406-9388
E-ISSN: 2580-8303

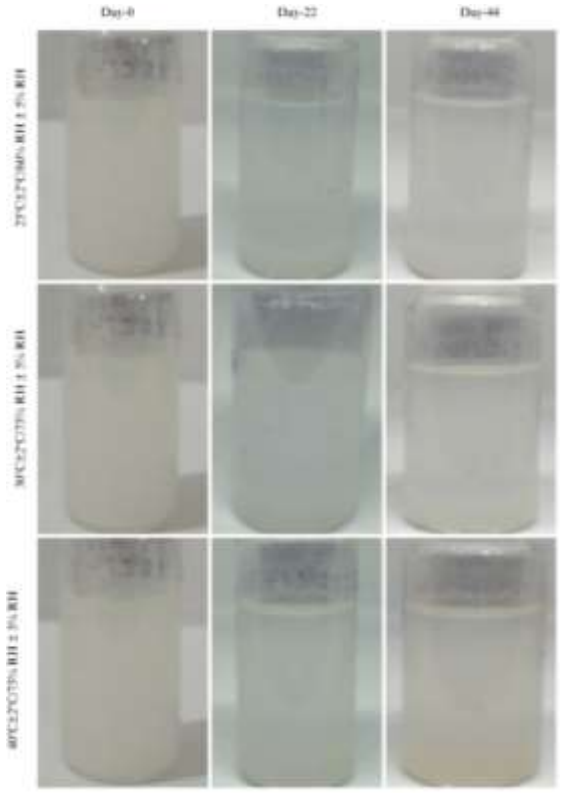

Figure 3. Results of organoleptic of the optimum formula stability test

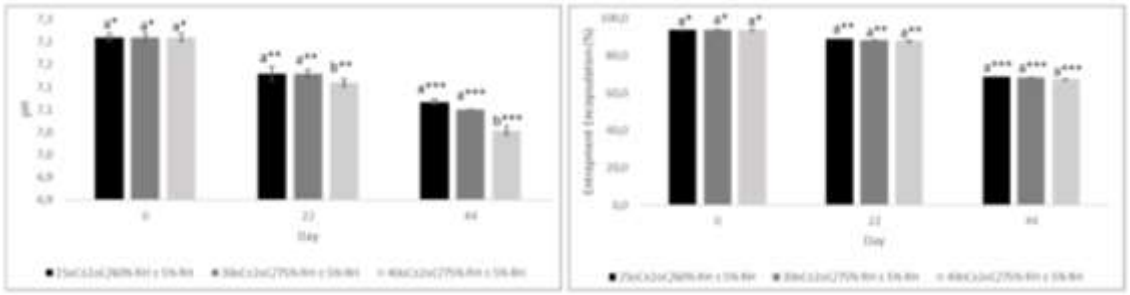

Note:
The notations "a" and "b" at each time point indicate a significant difference between the three storage conditions based on the Post Hoc-Duncan analysis ($p<0.05$).
The symbols *, **, and *** indicate significant differences between the storage conditions at each time point based on the Post Hoc-Duncan analysis ($p<0.05$).

Figure 4. Results of the pH and entrapment efficiency of the optimum formula stability test

The pH and entrapment efficiency of the optimum formula decreased over time, as depicted in Figure 4, correlating with storage temperature and humidity. A decrease in pH was observed in the optimized formula, which was attributed to the disruption of transethosome vesicles, which released free clindamycin. Clindamycin undergoes degradation upon liberation, which results in the release of H+ ions and a decrease in pH (Apriani et al., 2023). Additionally, the pH of the clindamycin HCl transethosome preparation was influenced by the phospholipon 90G used, which contains phosphatidylcholine. Hydrolysis of phosphatidylcholine produces phosphatidic acid, further lowering the pH (Hong et al., 2023). The optimum formula also showed a decrease in entrapment efficiency. High temperatures increase particle kinetic energy, leading to more collisions between vesicles and a faster reaction rate, which reduces entrapment efficiency (Salawu et al., 2023). Moreover, moisture accelerates the degradation of active ingredients through hydrolysis or oxidation, which can enhance drug release kinetics (Kamaly et al., 2016).

The shelf life of clindamycin HCl transethosomes is based on the release rate kinetics, and the observed release rate follows a zero-order kinetic model. According to Table 7 and Figure 5, the coefficient of

P-ISSN: 2406-9388
E-ISSN: 2580-8303

determination for this model was closest to 1, indicating a strong fit. The zero-order release kinetics imply that the drug's release rate remains constant over time, which is characteristic of systems where the active substance is uniformly dispersed and released at a steady rate, such as in suspension dispersion systems. This suggests that the formulation of clindamycin HCl transethosomes can maintain its release rate for a certain period without significant fluctuations.

The ICH Q1A(R2) guideline offers suggestions for estimating the shelf life of a product by considering the kinetics and storage conditions. The expiration life on the product label should be determined from real-time data if substantial changes are observed during the accelerated stability tests. This approach eliminates the need for six-month testing under accelerated conditions. In this study, extrapolation based on the Arrhenius equation was used to estimate the shelf life by correlating the kinetic constants with temperature, as shown in Table 8. The activation energy (Ea) of 2.978758 cal/mol indicates the minimum energy needed for the release reaction to occur. A lower Ea, which can result from extreme temperature and humidity, may accelerate the release rate due to increased molecular collisions.

Table 9 indicates that under typical storage conditions, the shelf life of clindamycin HCl transethosomes is estimated to be between 21-22 days. As expected, higher temperatures lead to a shorter shelf life, and at a lower temperature of 5°C, the extrapolated shelf life extends to 24.572 days. The study further highlights that preparations in suspension dispersion systems are less stable than those in solution forms, as undissolved particles in suspension can precipitate over time, leading to changes in the formulation's performance.

In conclusion, the shelf life of clindamycin HCl transethosomes is influenced by the temperature and storage conditions, with the Arrhenius equation providing a useful tool for extrapolating stability data. However, the nature of the formulation as a suspension system limits its stability compared to solution-based preparations.

Table 7. Optimum formula release rate kinetics

Release Rate Kinetics	25/60		30/75		40/75	
	R^2	k	R^2	k	R^2	k
Zero-Order	0.886	5.677	0.901	5.777	0.906	6.011
First-Order	0.8718	13.07476	0.8852	13.30506	0.8894	13.84417
Higuchi	0.5167	103.6596	0.6088	102.9963	0.4738	101.4435
Korsmeyer's Peppas	0.5683	0.00000119	0.5885	0.00000103	0.595	0.00000665
		n = 2.9813		n = 2.9812		n = 2.9816

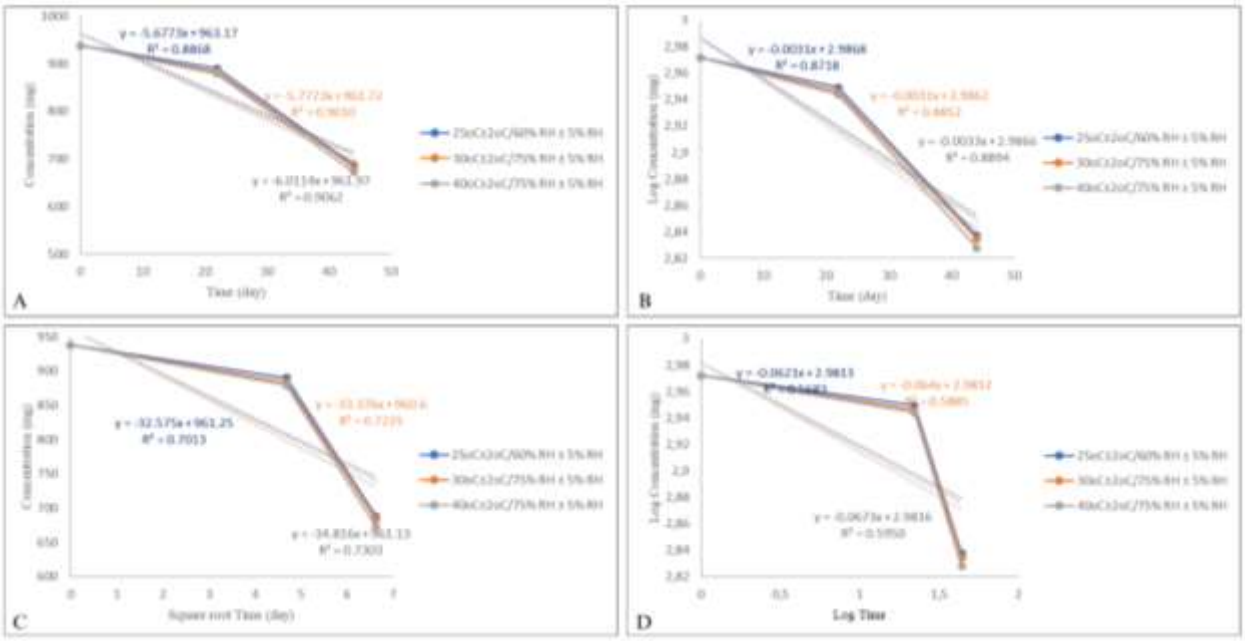

Figure 5. Release profile of optimum formula: A. zero-order, B. first-order, C. higuchi, D. korsmeyer-peppas

P-ISSN: 2406-9388
E-ISSN: 2580-8303

Table 8. Kinetic constants and parameters of the arrhenius in optimum formula

Storage Conditions (°C/%RH)	K	Log K	1/T(K^{-1})
25/60	6.011	0.7789	0.003356
30/75	5.777	0.7617	0.0033
40/75	5.677	0.7541	0.003195
Parameter of Arrhenius			
Ideal Gas Constant (R) (J $K^{-1}.mol^{-1}$)		$8.3134x10^{-3}$	
Arrhenius Factor (A)		13.84522	
Activation Energy (Ea) (cal/mol)		2.978758	

Table 9. Optimum formula shelf life

Storage Conditions (°C/%RH)	Shelf Life (t_{90}) (day)
25/60	22.536
30/75	22.093
40/75	21.274
5°C±3°C	24.572

CONCLUSION

The entrapment efficiency and particle size of clindamycin HCl transethosomes are substantially influenced by the concentrations of ethanol and Tween 80. By increasing the concentration of ethanol, the entrapment efficiency was reduced, and the particle size was larger. Conversely, the entrapment efficiency was reduced and the particle size was increased when the concentration of Tween 80 was increased. The optimum concentrations were determined to be 20% for ethanol and 15% for Tween 80. The clindamycin HCl transethosome formulation exhibited zero-order release kinetics, with an activation energy of 2.98 kcal/mol. The shelf life of the optimum formula was found to be 22.54 days at 25°C/60% RH and 24.57 days at 5°C, indicating the stability of the formulation under these conditions.

AUTHOR CONTRIBUTIONS

Conceptualization, E.F.A., A.A.; Methodology, E.F.A., A.A.; Software, E.F.A., A.A.; Validation, E.F.A., A.A., A.A.; Formal Analysis, E.F.A., A.A., A.A.; Investigation, M.A.M. F.A.; Resources, E.F.A., A.A.; Data Curation, M.A.M. F.A.; Writing - Original Draft, A.A.; Writing - Review & Editing, E.F.A., A.A.; Visualization, A.A.; Supervision, E.F.A., A.A.; Project Administration, E.F.A., A.A.; Funding Acquisition, E.F.A., A.A.

CONFLICT OF INTEREST

The authors declare that they have no conflicts of interest.

REFERENCES

Abdellatif, A. A., & Tawfeek, H. M. (2016). Transfersomal Nanoparticles for Enhanced Transdermal Delivery of Clindamycin. *AAPS PharmSciTech*; *17*; 1067–1074. doi: 10.1208/s12249-015-0441-7.

Abdulbaqi, I. M., Darwis, Y., Khan, N. A., Assi, R. A., & Khan, A. A. (2016). Ethosomal Nanocarriers: The Impact of Constituents and Formulation Techniques on Ethosomal Properties, In Vivo Studies, and Clinical Trials. *International Journal of Nanomedicine*; *11*; 2279–2304. doi: 10.2147/IJN.S105016.

Apriani, E. F., Mardiyanto, M., & Hendrawan, A. (2022). Optimization of Green Synthesis of Silver Nanoparticles from *Areca catechu* L. Seed Extract with Variations of Silver Nitrate and Extract Concentrations using Simplex Lattice Design Method. *Farmacia*; *70*; 917-924. doi: 10.31925/farmacia.2022.5.18.

Apriani, E. F., Rosana, Y., & Iskandarsyah, I. (2019). Formulation, Characterization, and In Vitro Testing of Azelaic acid Ethosome-Based Cream Against *Propionibacterium acnes* for the Treatment of Acne. *Journal of Advanced Pharmaceutical Technology & Research*; *10*; 75-80. doi: 10.4103/japtr.JAPTR_289_18.

Apriani, E. F., Shiyan, S., Hardestyariki, D., Starlista, V., & Febriani, M. (2023). Factorial Design for the Optimization of Clindamycin HCl-Loaded Ethosome with Various Concentration of Phospholipon 90G and Ethanol. Research Journal of Pharmacy and Technology, 16(4), 1561-1568. https://doi.org/10.52711/0974-360X.2023.00255

Ascenso, A., Raposo, S., Batista, C., Cardoso, P., Mendes, T., Praça, F. G., Bentley, M. V., & Simões, S. (2015). Development,

Characterization, and Skin Delivery Studies of Related Ultradeformable Vesicles: Transfersomes, Ethosomes, and Transethosomes. *International Journal of Nanomedicine*; *10*; 5837–5851. doi: 10.2147/IJN.S86186.

Bendas, E. R., & Tadros, M. I. (2007). Enhanced Transdermal Delivery of Salbutamol Sulfate Via Ethosomes. *AAPS PharmSciTech*; *8*; E107. doi: 10.1208/pt0804107.

Bnyan, R., Khan, I., Ehtezazi, T., Saleem, I., Gordon, S., O'Neill, F., & Roberts, M. (2018). Surfactant Effects on Lipid-Based Vesicle Properties. *Journal of Pharmaceutical Sciences*; *107*; 1237–1246. doi: 10.1016/j.xphs.2018.01.005.

Clancy, D., Hodnett, N., Orr, R., Owen, M., & Peterson, J. (2017). Kinetic Model Development for Accelerated Stability Studies. *AAPS PharmSciTech*; *18*; 1158–1176. doi: 10.1208/s12249-016-0565-4.

Dawson, A. L., & Dellavalle, R. P. (2013). Acne vulgaris. *BMJ (Clinical Research Ed.)*; *346*; f2634. doi: 10.1136/bmj.f2634.

Dlamini, N., Mukaya, H. E., Van Zyl, R. L., Chen, C. T., Zeevaart, R. J., & Mbianda, X. Y. (2019). Synthesis, Characterization, Kinetic Drug Release and Anticancer Activity of Bisphosphonates Multi-Walled Carbon Nanotube Conjugates. *Materials Science & Engineering C: Materials for Biological Applications*; *104*; 109967. doi: 10.1016/j.msec.2019.109967.

Dréno, B. (2017). What is New in the Pathophysiology of Acne, an Overview. *Journal of the European Academy of Dermatology and Venereology*; *31*; 8–12. doi: 10.1111/jdv.14374.

Elhalil, A., Tounsadi, H., Elmoubarki, R., Mahjoubi, F. Z., Farnane, M., Sadiq, M., Abdennouri, M., Qourzal, S., & Barka, N. (2016). Factorial Experimental Design for the Optimization of Catalytic Degradation of Malachite Green Dye in Aqueous Solution by Fenton Process. *Water Resources and Industry*; *15*; 41–48. doi: 10.1016/j.wri.2016.07.002.

El-Laithy, H. M., Shoukry, O., & Mahran, L. G. (2011). Novel Sugar Esters Proniosomes for Transdermal Delivery of Vinpocetine: Preclinical and Clinical Studies. *European Journal of Pharmaceutics and Biopharmaceutics*; *77*; 43–55.

Esposito, E., Calderan, L., Galvan, A., Cappellozza, E., Drechsler, M., Mariani, P., Pepe, A., Sguizzato, M., Vigato, E., Dalla Pozza, E., & Malatesta, M. (2022). Ex Vivo Evaluation of Ethosomes and Transethosomes Applied on Human Skin: A Comparative Study. *International Journal of Molecular Sciences*; *23*; 15112. doi: 10.3390/ijms232315112.

Ferrara, F., Benedusi, M., Sguizzato, M., Cortesi, R., Baldisserotto, A., Buzzi, R., Valacchi, G., & Esposito, E. (2022). Ethosomes and Transethosomes as Cutaneous Delivery Systems for Quercetin: A Preliminary Study on Melanoma Cells. *Pharmaceutics*; *14*; 1038. doi: 10.3390/pharmaceutics14051038.

Garg, V., Singh, H., Bhatia, A., Raza, K., Singh, S. K., Singh, B., & Beg, S. (2017). Systematic Development of Transethosomal Gel System of Piroxicam: Formulation Optimization, in Vitro Evaluation, and Ex Vivo Assessment. *AAPS PharmSciTech*; *18*; 58–71. doi: 10.1208/s12249-016-0489-z.

Hong, K., Yao, Q., Golding, J., Pristijono, P., Zhang, X., Hou, X., Yuan, D., Li, Y., Chen, L., Song, K., & Chen, J. (2023). Low Temperature Storage Alleviates Internal Browning of 'Comte de Paris' Winter Pineapple Fruit by Reducing Phospholipid Degradation, Phosphatidic Acid Accumulation and Membrane Lipid Peroxidation Processes. *Food Chemistry*; *404*; 134656. doi: 10.1016/j.foodchem.2022.134656.

ICH. (2003). Stability Testing of New Drug Substances and Products. Amsterdam: European Medicines Agency.

Iskandarsyah, I., Masrijal, C. D. P., & Harmita, H. (2020). Effects of Sonication on Size Distribution and Entrapment of Lynestrenol Transferosome. *International Journal of Applied Pharmaceutics*; *12*; 245–247. doi: 10.22159/ijap.2020.v12s1.FF053.

Kamaly, N., Yameen, B., Wu, J., & Farokhzad, O. C. (2016). Degradable Controlled-Release Polymers and Polymeric Nanoparticles: Mechanisms of Controlling Drug Release. *Chemical Reviews*; *116*; 2602–2663. doi: 10.1021/acs.chemrev.5b00346.

Kumar, M. K., Deep, K. C., Verma, S., Kumar, S. A., Kumar, D. D., Kashyap, P., & Prasad, M. S. (2019). Transethosomes and Nanoethosomes:

P-ISSN: 2406-9388
E-ISSN: 2580-8303

Recent Approach on Transdermal Drug Delivery System. London: IntechOpen.

Li, G., Fan, Y., Fan, C., Li, X., Wang, X., Li, M., & Liu, Y. (2012). Tacrolimus-loaded Ethosomes: Physicochemical Characterization and In Vivo Evaluation. *European Journal of Pharmaceutics and Biopharmaceutics*; *82*; 49–57. doi: 10.1016/j.ejpb.2012.05.011.

Lu, T., & Ten Hagen, T. L. M. (2020). A Novel Kinetic Model to Describe the Ultra-Fast Triggered Release of Thermosensitive Liposomal Drug Delivery Systems. *Journal of Controlled Release*; *324*; 669–678. doi: 10.1016/j.jconrel.2020.05.047.

Mardiyanto, M., Apriani, E. F., & Helyken, F. P. (2023). The Role of Temperature and pH in the Synthesis of Silver Nanoparticles using *Areca catechu* L. Seed Extract as Bioreductor. *Farmacia*; *71*; 244-253. doi: 10.31925/farmacia.2023.2.3.

Miksusanti, Apriani, E. F., & Bihurini, A. H. B. (2023). Optimization of Tween 80 and PEG-400 concentration in Indonesian Virgin Coconut Oil Nanoemulsion as Antibacterial Against *Staphylococcus aureus*. *Sains Malaysiana*; *52*; 1259-1272. doi: 10.17576/jsm-2023-5204-17.

Mollerup, S., Friis-Nielsen, J., Vinner, L., Hansen, T. A., Richter, S. R., Fridholm, H., Herrera, J. A., Lund, O., Brunak, S., Izarzugaza, J. M., Mourier, T., Nielsen, L. P., & Hansen, A. J. (2016). Propionibacterium Acnes: Disease-Causing Agent or Common Contaminant? Detection in Diverse Patient Samples by Next-Generation Sequencing. *Journal of Clinical Microbiology*; *54*; 980–987. doi: 10.1128/JCM.02723-15.

Monisha, C., Ganesh, G., Mythili, L., & Radhakrishnan, K. (2019). A Review on Ethosomes for Transdermal Application. *Research Journal of Pharmacy and Technology*; *12*; 3133-3143.

Pathan, I. B., Nandure, H., Syed, S. M., & Bairagi, S. (2016). Transdermal Delivery of Ethosomes as a Novel Vesicular Carrier for Paroxetine Hydrochloride: In Vitro Evaluation and In Vivo Study. *Marmara Pharmaceutical Journal*; *20*; 1–6. doi: 10.12991/mpj.201620113534.

Raj, A., Dua, K., Nair, R. S., Sarath Chandran, C., & Alex, A. T. (2023). Transethosome: An Ultra-Deformable Ethanolic Vesicle for Enhanced Transdermal Drug Delivery. *Chemistry and Physics of Lipids*; *255*; 105315. doi: 10.1016/j.chemphyslip.2023.105315.

Rakesh, R., & Anoop, K. R. (2012). Formulation and Optimization of Nano-Sized Ethosomes for Enhanced Transdermal Delivery of Cromolyn Sodium. *Journal of Pharmacy & Bioallied Sciences*; *4*; 333–340. doi: 10.4103/0975-7406.103274.

Salawu, S. O., & Okoya, S. S. (2023). Temperature Distribution and Thermal Criticality of Kinetics Exothermic Reactant in Concentric Cylinders Subject to Various Boundary Conditions. *ChemEngineering*; *7*; 19. doi: 10.3390/chemengineering7020019.

Somwanshi, S. B. (2019). Development and Evaluation of Novel Ethosomal Vesicular Drug Delivery System of *Sesamum indicum* L. Seed Extract. *Asian Journal of Pharmaceutics (AJP)*; *12*; 1282-S1290. doi: 10.22377/ajp.v12i04.2924.

Varia, U., Joshi, D., Jadeja, M., et al. (2022). Development and Evaluation of Ultradeformable Vesicles Loaded Transdermal Film of Boswellic Acid. *Futur Journal of Pharm Sciences*; *8*; 39. doi: 10.1186/s43094-022-00428-2.

Watkins, E. R., & Newbold, A. (2020). Factorial Designs Help to Understand How Psychological Therapy Works. *Frontiers in Psychiatry*; *11*; 429. doi: 10.3389/fpsyt.2020.00429.

Wu, P. S., Li, Y. S., Kuo, Y. C., Tsai, S. J., & Lin, C. C. (2019). Preparation and Evaluation of Novel Transfersomes Combined with the Natural Antioxidant Resveratrol. *Molecules*; *24*; 600. doi: 10.3390/molecules24030600.

Zeb, A., Qureshi, O. S., Kim, H. S., Cha, J. H., Kim, H. S., & Kim, J. K. (2016). Improved Skin Permeation of Methotrexate Via Nanosized Ultradeformable Liposomes. *International Journal of Nanomedicine*; *11*; 3813–3824. doi: 10.2147/IJN.S109565.

Zhou, Y., Wei, Y. H., Zhang, G. Q., & Wu, X. A. (2010). Synergistic Penetration of Ethosomes and Lipophilic Prodrug on The Transdermal Delivery of Acyclovir. *Archives of Pharmacal Research*; *33*; 567–574. doi: 10.1007/s12272-010-0411-2.

P-ISSN: 2406-9388
E-ISSN: 2580-8303